WILEY-VCH

FULL PAPER

Tuning Size and Geometry of Heteroleptic Coordination Cages by Variation of the Ligand Bent Angle

Ru-Jin Li, Farzaneh Fadaei-Tirani, Rosario Scopelliti, and Kay Severin*

[a] Dr. R.-J. Li, Dr. F. Fadaei-Tirani, Dr. R. Scopelliti, Prof. K. Severin
Institut des Sciences et Ingénierie Chimiques
École Polytechnique Fédérale de Lausanne (EPFL)
1015 Lausanne (Switzerland)
E-mail: kay.severin@epfl.ch

Supporting information for this article is given via a link at the end of the document.

Abstract: Spherical assemblies of type $[Pd_nL_{2n}]^{2n+}$ can be obtained from Pd^{II} salts and curved N-donor ligands L. It is well established that the bent angle α of the ligand is a decisive factor for the self-assembly process, with larger angles leading to complexes with a higher nuclearity *n*. Here, we report heteroleptic coordination cages of type $[Pd_nL_nL'_n]^{2n+}$, for which a similar correlation between the ligand bent angle and the nuclearity is observed. Tetranuclear cages were obtained by combining $[Pd(CH_3CN)_4](BF_4)_2$ with 1,3-di(pyridin-3-yl)benzene and ligands featuring a bent angle of α = 120 °. The utilization of a dipyridyl ligand with α = 149 ° led to the formation of a hexanuclear complex with a trigonal prismatic geometry, and for linear ligands, octanuclear assemblies of type $[Pd_8L_8L'_8]^{16+}$ were obtained. The predictable formation of heteroleptic Pd^{II} cages from 1,3-di(pyridin-3-yl)benzene and different dipyridyl ligands is evidence that there are entire classes of heteroleptic cage structures, which are privileged from a thermodynamic point of view

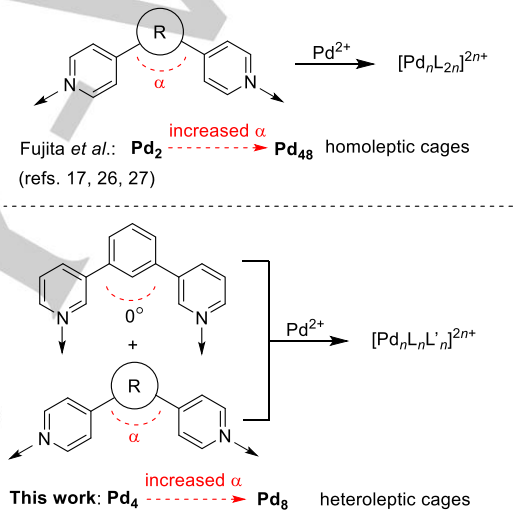

Scheme 1. The combination of di-4-pyridyl ligands with Pd^{II} salts gives complexes of the general formula $[Pd_nL_{2n}]^{2n+}$. Increasing the bent angle α leads to structures with a higher nuclearity *n*. Here, we show that a similar trend can be observed for heteroleptic cages.

Introduction

An appealing aspect of metallosupramolecular chemistry is the possibility to control the self-assembly process by ligand design. Important ligand characteristics are size, geometry, rigidity, nature of the donor atoms, denticity, charge, and steric demand. All these parameters may influence the self-assembly reaction.[1-11] Evidently, the reaction partner needs to be taken into account, and the ligand should be a good match for the corresponding metal ion (or complex).

For the construction of Pd^{II}-based metal-ligand assemblies, polydentate N-donor ligands were found to be well suited.[12-17] Elaborate polypyridyl ligands were used to build complex molecular architectures,[18-25] but even simple di-4-pyridyl ligands can give rise to assemblies with up to 48 Pd^{II} ions.[26] A crucial design element for di-4-pyridyl ligands is the bent angle α between the two coordinate vectors of the pyridyl groups (Scheme 1). The nuclearity *n* of the final assembly is dependent on α, with more straight ligands (higher α) favoring the formation of complexes with a higher nuclearity. The bent angle is particularly relevant for coordination cages of the formula $[Pd_nL_{2n}]^{2n+}$, which can be obtained by combination of di-4-pyridyl ligands with Pd^{II} salts.[17] For these assemblies, even subtle changes in α can lead to abrupt changes in the nuclearity *n*.[27]

Below, we show that the bent angle α can also be used to control the nuclearity of *heteroleptic* coordination cages. A slight increase of α from 120 ° to 149 resulted in a complete structural switch from a tetranuclear $[Pd_4L_4L'_4]^{8+}$ complex to a hexanuclear $[Pd_6L_6L'_6]^{12+}$ complex. Furthermore, we were able to observe unprecedented octanuclear $[Pd_8L_8L'_8]^{16+}$ complexes for linear ligands with α = 180 °. The results show that there are entire families of heteroleptic cages complexes, which are privileged from a thermodynamic point of view.

Results and Discussion

Cage-like structures of the formula $[Pd_nL_{2n}]^{2n+}$ have been investigated extensively over the last years, and applications in medicinal chemistry,[28-36] catalysis,[37-41] and materials science[42-47] and have emerged. Most of the $[Pd_nL_{2n}]^{2n+}$

complexes reported to date display high symmetry. Low-symmetry assemblies could show interesting new properties. For example, they might be better hosts for guest molecules, which likewise display low symmetry. In the case of heteroleptic assemblies, the presence of different ligands could be used to introduce different functional groups.

Several groups have started to investigate such low-symmetry Pd assemblies. Two synthetic strategies have been explored in this context: a) the utilization of ligands with reduced symmetry (e.g. lack of C_2 symmetry),[18,48-51] and b) the controlled formation of heteroleptic assemblies using two different ligands.[52-55] The latter strategy has resulted in the discovery of several mixed-ligand assemblies of the general formula $[Pd_nL_xL'_y]^{2n+}$ ($x + y = 2n$). Most of these heteroleptic assemblies contain two Pd^{2+} ions,[56-62] and there are only few examples of structurally defined mixed-ligand assemblies with $n > 2$.[63-67] We have recently reported a $[Pd_6L_6L'_6]^{12+}$ complex, which was identified in a competition experiment using a set of six different dipyridyl ligands.[63] The hexanuclear complex was found to display high thermodynamic stability, outcompeting several homoleptic complexes. Intrigued by this finding, we have embarked in a more systematic investigation of heteroleptic $[Pd_nL_xL'_y]^{2n+}$ complexes. While investigating other L/L' ligand combinations, we found that a mixture of the di-3-pyridyl ligand **L1**, the di-4-pyridyl ligand **L2**, and $[Pd(CH_3CN)_4](BF_4)_2$ in acetonitrile gave rise to a defined tetranuclear cage complex of the formula $[Pd_4(\mathbf{L1})_4(\mathbf{L2})_4]^{8+}$ (Scheme 2). The new assembly was characterized by NMR spectroscopy, high-resolution mass spectrometry (HRMS), and single crystal X-ray diffraction (for details, see Supporting Information, SI).

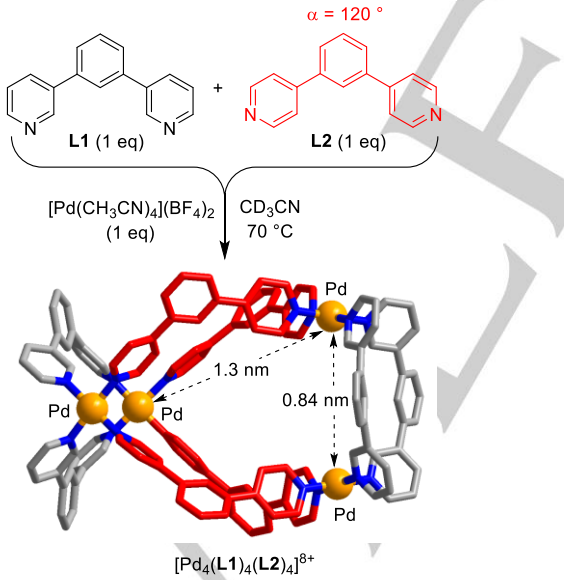

Scheme 2. Synthesis of the heteroleptic cage $[Pd_4(\mathbf{L1})_4(\mathbf{L2})_4]^{8+}$. The structure of the product is based on a crystallographic analysis.

The Pd^{2+} ions in $[Pd_4(\mathbf{L1})_4(\mathbf{L2})_4]^{8+}$ are positioned at the vertices of a distorted tetrahedron, with four long (Pd···Pd = 1.3 nm) and two short edges (Pd···Pd = 0.84 nm). The structure can be deconstructed into two macrocyclic $[Pd_2(\mathbf{L1})_2]^{4+}$ fragments, which are connected by four ligands **L2**. To the best of our knowledge, this structural motif has not been reported before for heteroleptic $[Pd_nL_xL'_y]^{2n+}$ complexes.

The synthesis of $[Pd_4(\mathbf{L1})_4(\mathbf{L2})_4]^{8+}$ was performed at elevated temperature (70 °C) for a prolonged period of time (overnight). Therefore, we assumed that the complex was formed under thermodynamic control. To corroborate this hypothesis, we equilibrated a mixture of the corresponding homoleptic complexes $[Pd_2(\mathbf{L1})_4]^{4+}$ (6 eq) and $[Pd_{12}(\mathbf{L2})_{24}]^{24+}$ (1 eq) in CD_3CN at 70 °C (Scheme 3a). Analysis of the mixture by ^1H NMR spectroscopy revealed formation of the heteroleptic cage $[Pd_4(\mathbf{L1})_4(\mathbf{L2})_4]^{8+}$. However, due to the kinetic inertness of $[Pd_{12}(\mathbf{L2})_{24}]^{24+}$,[68] the rearrangement was very slow, and small amounts of the homoleptic cages could still be observed after 70 days (SI, Figure S35). A significantly faster rearrangement was observed when ligand **L2** (4 eq) was added to a solution of $[Pd_2(\mathbf{L1})_4]^{4+}$ (1 eq) (Scheme 3b). Within 4 h (70 °C), a complete transformation of $[Pd_2(\mathbf{L1})_4]^{4+}$ into the heteroleptic cage $[Pd_4(\mathbf{L1})_4(\mathbf{L2})_4]^{8+}$ was observed (for details, see SI, Figure S36).[69] Taken together, the results are strong evidence that $[Pd_4(\mathbf{L1})_4(\mathbf{L2})_4]^{8+}$ is formed under thermodynamic control.

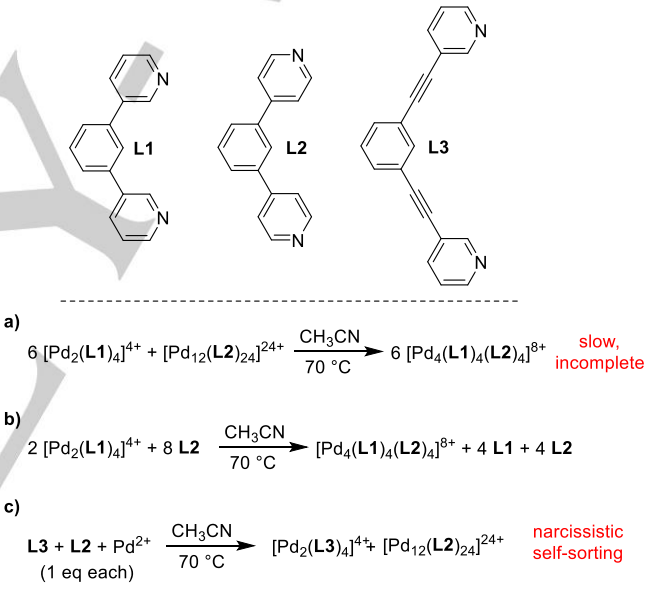

Scheme 3. Formation of $[Pd_4(\mathbf{L1})_4(\mathbf{L2})_4]^{8+}$ by ligand exchange reactions (a and b), and narcissistic self-sorting with the ligand combination **L3**/**L2** (c).

The preferential formation of the heteroleptic cage $[Pd_4(\mathbf{L1})_4(\mathbf{L2})_4]^{8+}$ over the homoleptic cages $[Pd_2(\mathbf{L1})_4]^{4+}$ and $[Pd_{12}(\mathbf{L2})_{24}]^{24+}$ is likely related to the enthalpy of the system, because there is no strong bias from a translational entropy point-of-view (see equation in Scheme 3a). Further information was obtained by an experiment using ligand **L3** instead of **L1** (Scheme 3). **L3** represents a structural analogue of **L1**. Similar to **L1**, it forms a dinuclear cage when combined with Pd^{2+}.[70] Interestingly, the reaction between equimolar amounts of **L3**, **L2**, and $[Pd(CH_3CN)_4](BF_4)_2$ resulted in complete narcissistic self-sorting (Scheme 3c & SI, Figure S39), as opposed to the integrative self-sorting observed for the ligand combination **L1**/**L2** (Scheme 2).[54,55,71,72] We have modelled the structure of the hypothetical heteroleptic cage $[Pd_4(\mathbf{L2})_4(\mathbf{L3})_4]^{4+}$ computationally, and we were not able to detect any particular strain in the system (SI, Figure S46a). Therefore, we suspected that the different

outcome of reactions with the ligand combinations **L1**/**L2** vs. **L3**/**L2** was related to the relative stability of the homoleptic complexes $[Pd_2(\mathbf{L1})_4]^{4+}$ and $[Pd_2(\mathbf{L3})_4]^{4+}$.

The solid state structure of $[Pd_2(\mathbf{L1})_4]^{4+}$ had not been reported before. A crystallographic analysis of a related complex with four methoxy substituents had been described by the Johnson group, but the quality of the data was poor. Therefore, we have examined the structure of $[Pd_2(\mathbf{L1})_4](NO_3)_2$ by single crystal X-ray diffraction (the NO_3^- counter ion facilitated crystallization). A graphic representation of the cationic cage is depicted in Figure 1. The two Pd^{2+} ions display a square planar coordination environment with an eclipsed arrangement of the N-donor atoms. The distance between the Pd^{2+} ions is 0.74 nm. This value is significantly shorter than the 0.84 nm observed for the $[Pd_2(\mathbf{L1})_2]^{4+}$ fragments in $[Pd_4(\mathbf{L1})_4(\mathbf{L2})_4]^{8+}$ (Scheme 1). It is also noteworthy that the planes defined by the square planar $Pd(py)_4$ groups in $[Pd_4(\mathbf{L1})_4(\mathbf{L2})_4]^{8+}$ are inclined by 22 ° (SI, Figure S45), in contrast to the co-planar arrangement of the $Pd(py)_4$ groups in $[Pd_2(\mathbf{L1})_4]^{4+}$. The more compact geometry of $[Pd_2(\mathbf{L1})_4]^{4+}$ points to an intrinsic strain (intra-ligand and/or charge-charge repulsion) for this homoleptic cage.

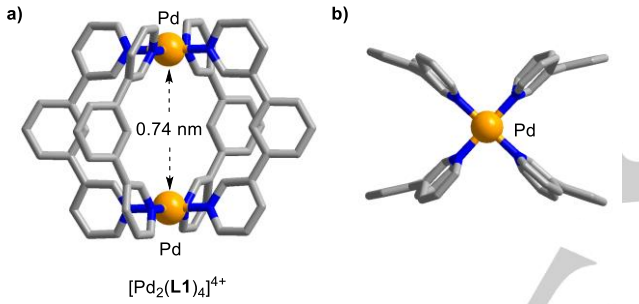

Figure 1. Molecular structure of the homoleptic cage $[Pd_2(\mathbf{L1})_4]^{4+}$ in the crystal with view from the side (**a**) and along the Pd···Pd axis (**b**).

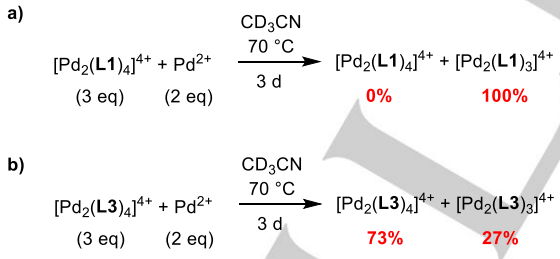

Scheme 4. The addition of $[Pd(CH_3CN)_4](BF_4)_2$ (2 eq) to $[Pd_2(\mathbf{L1})_4]^{4+}$ leads to complete rearrangement to the bowl-shaped complex $[Pd_2(\mathbf{L1})_3]^{4+}$ (**a**). For $[Pd_2(\mathbf{L3})_4]^{4+}$, only a small amount of rearranged complex is observed (**b**).

Additional evidence for strain in $[Pd_2(\mathbf{L1})_4]^{4+}$ was obtained by solution-based experiments (Scheme 4). When $[Pd(CH_3CN)_4](BF_4)_2$ (2 eq) was added to a solution of $[Pd_2(\mathbf{L1})_4]^{4+}$ (3 eq) in CD_3CN, a quantitative rearrangement into the bowl-shaped complex $[Pd_2(\mathbf{L1})_3]^{4+}$ was observed by NMR spectroscopy (the fourth coordination site at Pd is probably occupied by acetonitrile).[73,74] This result indicates that ligand displacement in $[Pd_2(\mathbf{L1})_4]^{4+}$ is facile. In contrast, when a similar experiment was performed with $[Pd_2(\mathbf{L3})_4]^{4+}$, only partial rearrangement was observed, and the dominant Pd species in solution was still $[Pd_2(\mathbf{L3})_4]^{4+}$ (Scheme 4b). The reduced strain in $[Pd_2(\mathbf{L3})_4]^{4+}$, when compared to $[Pd_2(\mathbf{L1})_4]^{4+}$, could be due to the increased flexibility of the longer ligand **L3**. Furthermore, the alkynyl spacers abolish unfavorable steric interactions between the pyridyl rings and the central phenylene spacer. Overall, the results suggest that **L1** is predisposed to form heteroleptic complexes, because the homoleptic complex $[Pd_2(\mathbf{L1})_4]^{4+}$ suffers from intrinsic strain. Therefore, we have examined reactions of Pd^{2+} with **L1** and other dipyridyl ligands.

First, we have investigated a reaction using **L4** (Scheme 5). Similar to **L2**, the coordinate vectors of **L4** form an angle of 120 °. Equilibration of a mixture of **L1** (1 eq), **L4** (1 eq), and $[Pd(CH_3CN)_4](BF_4)_2$ (1 eq) in CD_3CN resulted in the clean formation of the heteroleptic cage $[Pd_4(\mathbf{L1})_4(\mathbf{L4})_4]^{8+}$, as evidenced by NMR spectroscopy and HRMS. Single crystals were obtained by vapor diffusion of 2-isopropoxypropane into a CH_3CN solution of the cage, and a crystallographic analysis was performed. The results showed that the structure of $[Pd_4(\mathbf{L1})_4(\mathbf{L4})_4]^{8+}$ is similar to what was observed for $[Pd_4(\mathbf{L1})_4(\mathbf{L2})_4]^{8+}$: two macrocyclic $[Pd_2(\mathbf{L1})_2]^{4+}$ fragments are bridged by four ligands **L4** (Scheme 5). Due to the increased length of **L4**, when compared to **L2**, the tetrahedral arrangement of the Pd^{2+} ions is even more distorted, with long Pd···Pd distances of 1.6 nm, and short Pd···Pd distances of 0.84 nm.

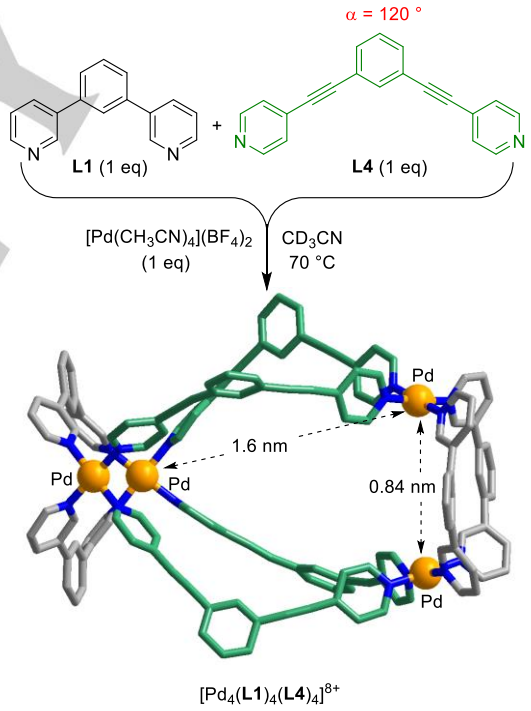

Scheme 5. Synthesis of the heteroleptic cage $[Pd_4(\mathbf{L1})_4(\mathbf{L4})_4]^{8+}$. The structure of the product is based on a crystallographic analysis.

Next, we have examined reactions with the thiophenyl-bridged ligand **L5** (Scheme 6). This ligand displays a bent angle of α = 149 °.[27] Heating a mixture of **L1** (1 eq), **L5** (1 eq), and $[Pd(CH_3CN)_4](BF_4)_2$ (1 eq) in CD_3CN to 70 °C for 7 days gave again a defined assembly, as evidenced by ^1H and DOSY NMR spectroscopy (SI, Figure S23–S26). However, the HRMS data suggested that a hexanuclar instead of a tetranuclear complex

had formed (SI, Figure S27). The molecular structure of $[Pd_6(\mathbf{L1})_6(\mathbf{L5})_6]^{12+}$ was established by single crystal X-ray diffraction (Scheme 6). The six Pd^{2+} ions are positioned at the vertices of a trigonal prism.[65] The edges of the two triangular faces of the prism are occupied by **L5**, whereas the height of the prism is determined by **L1**. As for the tetranuclear cages, one can observe the presence of macrocyclic $[Pd_2(\mathbf{L1})_2]^{4+}$ fragments. The average Pd···Pd distance in these macrocycles is 0.81 nm. This value is slightly shorter than what was found for the tetranuclear cages $[Pd_4(\mathbf{L1})_4(\mathbf{L2})_4]^{8+}$ and $[Pd_4(\mathbf{L1})_4(\mathbf{L4})_4]^{8+}$, but still larger than what was observed for the homoleptic complex $[Pd_2(\mathbf{L1})_4]^{4+}$.

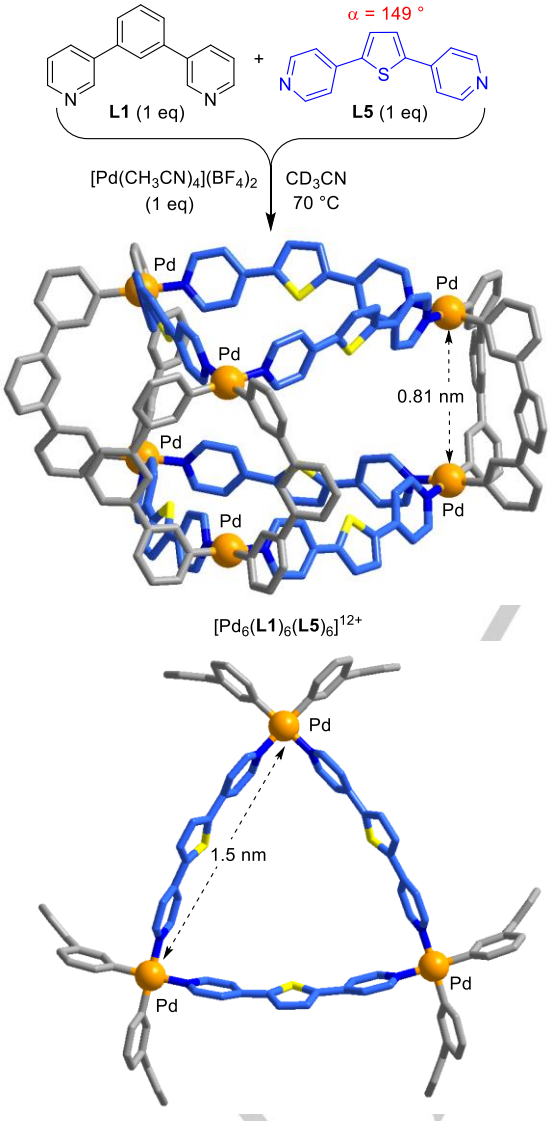

Scheme 6. Synthesis of the heteroleptic cage $[Pd_6(\mathbf{L1})_6(\mathbf{L5})_6]^{12+}$. The structure of the product is based on a crystallographic analysis (view from the side and from the top).

The result obtained with **L5** suggested that the ligand bent angle can have a profound influence on the outcome of the self-assembly process. Therefore, we subsequently investigated a reaction involving the linear dipyridyl ligand **L6** (Scheme 7). Analysis of the equilibrated reaction mixture by ^1H and DOSY NMR spectroscopy revealed the formation of a new assembly (SI, Figure S28–30). The dominant peaks in the HRMS spectrum of the reaction mixture could be attributed to an octanuclear complex of the formula $[\{Pd_8(\mathbf{L1})_8(\mathbf{L6})_8\}(BF_4)_n]^{(16-n)+}$ (Figure 2a). Attempts to characterize this complex by single crystal X-ray diffraction were unfortunately not successful. We were able to obtain single crystals, but the diffraction data was always poor. In analogy to what was observed for the heteroleptic complexes described above, we assume that $[Pd_8(\mathbf{L1})_8(\mathbf{L6})_8]^{16+}$ is composed of $[Pd_2(\mathbf{L1})_2]^{4+}$ macrocycles, which are bridged by **L6**. This connectivity would result in the formation of a tetragonal prismatic structure, and a molecular model (*MMFF*) of this structure is depicted in Figure 2b.

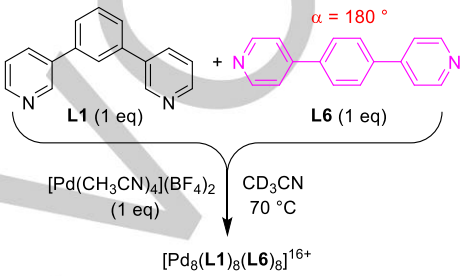

Scheme 7. Synthesis of the heteroleptic cage $[Pd_8(\mathbf{L1})_8(\mathbf{L6})_8]^{16+}$.

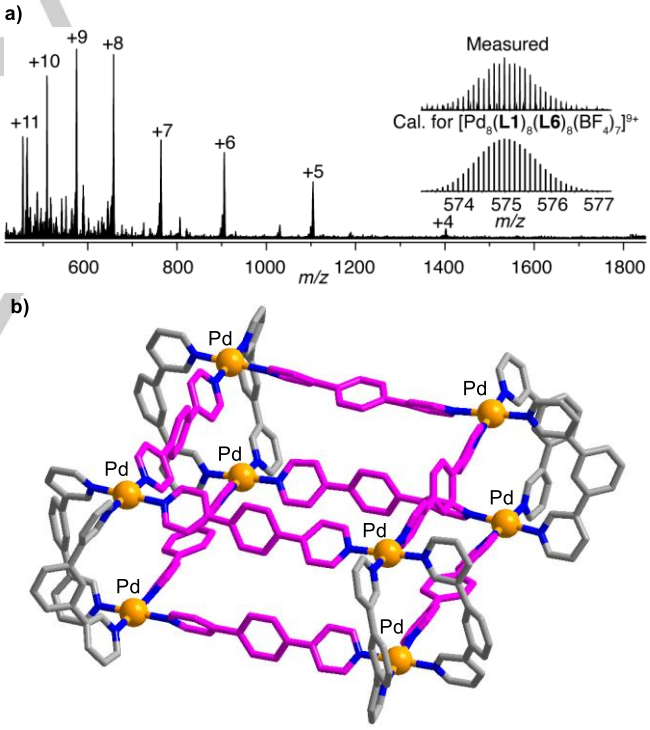

Figure 2. HRMS of $[\{Pd_8(\mathbf{L1})_8(\mathbf{L6})_8\}(BF_4)_x]^{(16-x)+}$ (**a**), and molecular model (MMFF) of the proposed structure (**b**).

The incorporation of alkynyl spacers into linear dipyridyl ligands renders them more flexible, and bent angles well below 180 ° can be attained.[75] To examine the effect of increased ligand flexibility, we have investigated the reaction between **L1**, $[Pd(CH_3CN)_4](BF_4)_2$, and the extended dipyridyl ligand **L7**

(Scheme 8). In contrast to what was observed for reactions with the ligand combinations **L1**/**L2**, **L1**/**L4**, **L1**/**L5**, and **L1**/**L6**, the mixture of **L1** and **L7** did not result in the formation of a defined product. Instead, two sets of ligand signals were observed in the ^{1}H NMR spectrum (ratio: 4 : 3, SI, Figure S32), and the DOSY NMR spectrum indicated that two assemblies with distinct sizes had formed (SI, Figure S33). An explanation for the NMR data was obtained by a HRMS analysis. The mass spectrum showed peaks corresponding to a hexanuclear *and* an octanuclear complex (SI, Figure S34). In light of the previous results, we assume that these assemblies have a trigonal and a tetragonal prismatic structure (Scheme 8). The relative ratio between $[Pd_6(\mathbf{L1})_6(\mathbf{L7})_6]^{12+}$ and $[Pd_8(\mathbf{L1})_8(\mathbf{L7})_8]^{16+}$ could be influenced by the concentration of the building blocks. When the reaction was performed under dilute concentrations ([Pd] = 0.9 mM), the hexanuclear complex $[Pd_6(\mathbf{L1})_6(\mathbf{L7})_6]^{12+}$ was the dominating product, and only small peaks for $[Pd_8(\mathbf{L1})_8(\mathbf{L7})_8]^{16+}$ could be observed in the ^{1}H NMR spectrum (SI, Figure S42).

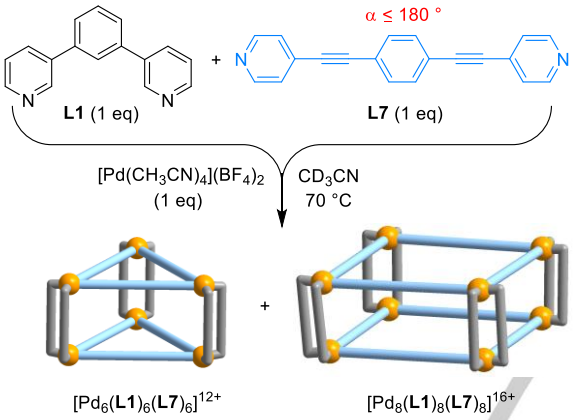

Scheme 8. The combination of **L1**, **L7**, and $[Pd(CH_3CN)_4](BF_4)_2$ results in the formation of a mixture of the heteroleptic complexes $[Pd_6(\mathbf{L1})_6(\mathbf{L7})_6]^{12+}$ and $[Pd_8(\mathbf{L1})_8(\mathbf{L7})_8]^{16+}$.

The results described above are evidence that ligand **L1** is prone to form heteroleptic assemblies. A common structural pattern is the presence of macrocyclic $[Pd_2(\mathbf{L1})_2]^{4+}$ fragments, which are bridged by different ditopic pyridyl ligands. To further test the robustness of this structural motif, we have examined a ligand exchange reaction (Scheme 9). A solution of the tetranuclear cage $[Pd_4(\mathbf{L1})_4(\mathbf{L4})_4]^{8+}$ in CD_3CN was prepared as described above. Subsequently, 4 equivalents of **L2** were added. Ligand **L2** is more basic than **L4**,[76] and thus a better N-donor ligand. After heating the mixture at 70 °C for 12 h, we observed the clean conversion of $[Pd_4(\mathbf{L1})_4(\mathbf{L4})_4]^{8+}$ into the smaller cage $[Pd_4(\mathbf{L1})_4(\mathbf{L2})_4]^{8+}$, with concomitant liberation of **L4** (Scheme 9). We would like to add that ligand basicity seems to be the main driving force for the conversion of $[Pd_4(\mathbf{L1})_4(\mathbf{L4})_4]^{8+}$ into $[Pd_4(\mathbf{L1})_4(\mathbf{L2})_4]^{8+}$, but other factors such as solvation or anion effects can play a role as well.

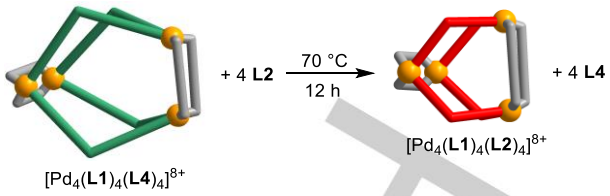

Scheme 9. Cage-to-cage conversion by ligand exchange.

Finally, we were interested if the preferential formation of heteroleptic complexes would be affected by the donor strength of the key building block **L1**. Therefore, we have examined reactions with ligand **L8**, featuring two electron-donating methoxy groups in *para* position to the N-donor atoms. Equilibration (70 °C, 12 h) of a mixture of **L2**, **L8**, and $[Pd(CH_3CN)_4](BF_4)_2$ led to the clean formation of the heteroleptic cage $[Pd_4(\mathbf{L2})_4(\mathbf{L8})_4]^{8+}$. A crystallographic analysis showed that the solid state structure of $[Pd_4(\mathbf{L2})_4(\mathbf{L8})_4]^{8+}$ is very similar to that of $[Pd_4(\mathbf{L1})_4(\mathbf{L2})_4]^{8+}$, with Pd···Pd distances of 1.3 and 0.81 nm (Scheme 10). Apparently, the formation of heteroleptic cages by integrative self-sorting is not influenced substantially by ligand basicity, at least in this particular case.

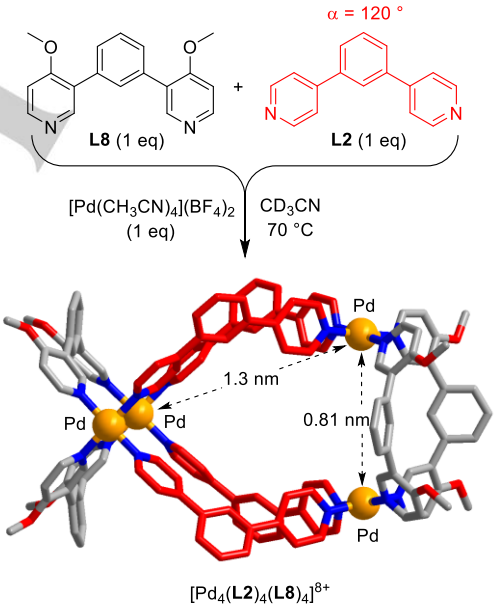

Scheme 10. Synthesis of the heteroleptic cage $[Pd_4(\mathbf{L2})_4(\mathbf{L8})_4]^{8+}$. The structure of the product is based on a crystallographic analysis.

Conclusion

The design of structurally defined $[Pd_nL_nL'_n]^{2n+}$ complexes is a challenging task, and only few examples have been reported to date.[56-67] A key difficulty is the identification of a ligand combination L/L', which favors the formation of a particular heteroleptic complex over homoleptic complexes and alternative mixed-ligand assemblies. Herein, we have described an entire new class of $[Pd_nL_nL'_n]^{2n+}$ complexes, with different sizes and geometries. The common feature of these complexes is the presence of the dipyridyl ligand **L1**, which shows a high propensity

to form heteroleptic complexes containing macrocyclic $[Pd_2(\mathbf{L1})_2]^{4+}$ fragments. By variation of the bent angle α of the second ligand L', we were able to increase the nuclearity *n* of the assembly from 4 to 8. The tetranuclear complex $[Pd_4(\mathbf{L1})_4(\mathbf{L4})_4]^{8+}$ can undergo a ligand exchange reaction without alteration of the main geometry, underlining the resilience of this structural motif. Control experiments and structural data suggest that the preferential formation of heteroleptic $[Pd_n(\mathbf{L1})_nL'_n]^{2n+}$ complexes is enabled by the intrinsic strain of the homoleptic complex $[Pd_2(\mathbf{L1})_4]^{4+}$. Overall, our represent an important advance in establishing the design rules for mixed-ligand assemblies, a field which is still in its infancy.

Acknowledgements

The work was supported by the École Polytechnique Fédérale de Lausanne (EPFL). We thank Dr. Daniel Ortiz for measuring mass spectra.

Keywords: Supromolecular Chemistry • Coordination Cages • Heteroleptic Cages • Pyridyl Ligands • Palladium

[1] S. Lee, H. Jeong, D. Nam, M. S. Lah, W. Choe, *Chem. Soc. Rev*. **2021**, *50*, 528–555.
[2] E. J. Gosselin, C. A. Rowland, E. D. Bloch, *Chem. Rev.* **2020**, *120*, 8987–9014.
[3] M. Hardy, A. Lützen, *Chem. Eur. J.* **2020**, *26*, 13332–13346.
[4] S. Chakraborty, G. R. Newkome, *Chem. Soc. Rev.*, **2018**, *47*, 3991–4016.
[5] M. D. Ward, C. A. Hunter, N. H. Williams, *Acc. Chem. Res.* **2018**, *51*, 2073–2147.
[6] S. M. Jansze, K. Severin, *Acc. Chem. Res.* **2018**, *51*, 2139–2082.
[7] L.-J. Chen, H.-B. Yang, M. Shionoya, *Chem. Soc. Rev.* **2017**, *46*, 2555–2567.
[8] A. M. Lifschitz, M. S. Rosen, C. M. McGuik, C. A. Mirkin, *J. Am. Chem. Soc.* **2015**, *137*, 7252–7261
[9] T. R. Cook, P. J. Stang, *Chem. Rev*. **2015**, *115*, 7001–7045.
[10] T. K. Ronson, S. Zarra, S. P. Black, J. R. Nitschke, *Chem. Commun.* **2013**, *49*, 2476–2490.
[11] R. Chakrabarty, P. S. Mukherjee, P. J. Stang, *Chem. Rev.* **2011**, *111*, 6810–6918.
[12] S. Saha, I. Regeni, G. H. Clever, *Coord. Chem. Rev.* **2018**, *374*, 1–14.
[13] R. A. S. Vasdev, D. Preston, J. D. Crowley, *Chem. Asian J.* **2017**, *12*, 2513–2523.
[14] G. H. Clever, P. Punt, *Acc. Chem. Res.* **2017**, *50*, 2233–2243.
[15] M. Han, D. M. Engelhard, G. H. Clever, *Chem. Soc. Rev.* **2014**, *43*, 1848–1860.
[16] S. Mukherjee, P. S. Mukherjee, *Chem. Commun.* **2014**, *50*, 2239–2248.
[17] K. Harris, D. Fujita, M. Fujita, *Chem. Commun.* **2013**, *49*, 6703–6712.
[18] S. Samantray, S. Krishnaswarmy, D. K. Chand, *Nat. Commun.* **2020**, *11*, 880.
[19] K. Wu, B. Zhang, C. Drechsler, J. J. Holstein, G. H. Clever, *Angew. Chem. Int. Ed.* **2021**, *59*, DOI: 10.1002/anie.202012425.
[20] Y. Tamura, H. Takezawa, M. Fujita, *J. Am. Chem. Soc.* **2020**, *142*, 5504–5508.
[21] D. Preston, J. E. M. Lewis, J. D. Crowley. *J. Am. Chem. Soc.* **2017**, *139*, 2379–2386.
[22] K. Yazaki, M. Akita, S. Prusty, D. K. Chand, T. Kikuchi, H. Sato, M. Yoshizawa, *Nat. Commun.* **2017**, *8*, 15914.
[23] G. Cecot, M. Marmier, S. Geremia, R. De Zorzi, A. V. Vologzhanina, P. Pattison, E. Solari, F. Fadaei Tirani, R. Scopelliti, K. Severin, *J. Am. Chem. Soc.* **2017**, *139*, 8371–8381.
[24] I. A. Bhat, D. Samanta, P. S. Mukherjee, *J. Am. Chem. Soc.* **2015**, ***137***, 9497–9502.
[25] Q.-F. Sun, S. Sato, M. Fujita, *Nat. Chem.* **2012**, *4*, 330–333.
[26] D. Fujita, Y. Ueda, S. Sato, N. Mizuno, T. Kumasaka, M. Fujita, *Nature* **2016**, ***540***, 563–566.
[27] Q.-F. Sun, J. Iwasa, D. Ogawa, Y. Ishido, S. Sato, T. Ozeki, Y. Sei, K. Yamaguchi, M. Fujita, *Science* **2010**, *328*, 1144–1147.
[28] B. Woods, R. D. M. Silva, C. Schmidt, D. Wragg, M. Cavaco, V. Neves, V. F. C. Ferreira, L. Gano, T. S. Morais, F. Mendes, J. D. G. Correira, A. Casini, *Bioconjugate Chem.* **2021**, DOI: 10.1021/acs.bioconjchem.0c00659.
[29] J. Liu, T. Luo, Y. Xue, L. Mao, P. J. Stang, M. Wang, *Angew. Chem. Int. Ed.* **2021**, DOI: 10.1002/anie.202013904.
[30] R. A. S. Vasdev, L. F. Gaudin, D. Preston, J. P. Jogy, G. I. Giles, J. D. Crowley, *Front. Chem.* **2018**, *6*, 563
[31] A. Casini, B. Woods, M. Wenzel, *Inorg. Chem.* **2017**, *56*, 14715–14729.
[32] F. Kaiser, A. Schmidt, W. Heydenreuter, P. J. Altmann, A. Casini, S. A. Sieber, F. E. Kühn, *Eur. J. Inorg. Chem.* **2016**, 5189–5196.
[33] A. Schmidt, M. Hollering, M. Drees, A. Casini, F. E. Kühn, *Dalton Trans.* **2016**, *45*, 8556–8565.
[34] A. Schmidt, V. Molano, M. Hollering, A. Pöthig, A. Casini, F. E. Kühn, *Chem. Eur. J.* **2016**, *22*, 2253–2256.
[35] S. M. McNeill, D. Preston, J. E. M. Lewis, A. Robert, K. Knerr-Rupp, D. O. Graham, J. R. Wright, G. I. Giles, J. D. Crowley, *Dalton Trans.* **2015**, *44*, 11129–11136.
[36] J. E. M. Lewis, E. L. Gavey, S. A. Cameron, J. D. Crowley, *Chem. Sci.* **2012**, *3*, 778–784.
[37] Y. Xue, X. Hang, J. Ding, B. Li, R. Zhu, H. Pang, Q. Xu, *Coord. Chem. Rev.* **2021**, *430*, 213656.
[38] A. B. Grommet, M. Feller, R. Klajn, *Nat. Nanotech.* **2020**, *15*, 256–271.
[39] A. C. H. Jans, X. Caumes, J. N. H. Reek, *ChemCatChem* **2019**, *11*, 287–297.
[40] L. J. Jongkind, X. Caumes, A. P. T. Hartendorp, J. N. H. Reek, *Acc. Chem. Res.* **2018**, *51*, 2115–2128.
[41] I. Sinha, P. S. Mukherjee, *Inorg. Chem.* **2018**, *57*, 4205–4221.
[42] S. Datta, M. L. Saha, P. J. Stang, *Acc. Chem. Res.* **2018**, *51*, 2047–2063.
[43] K. C. Bentz, S. M. Cohen, *Angew. Chem. Int. Ed.* **2018**, *57*, 14992–15001.
[44] Y. Gu, E. A. Alt, H. Wang, X. Li, A. P. Willard, J. A. Johnson, *Nature* **2018**, *560*, 65–69.
[45] Y. Wang, Y. Gu, E. G. Keeler, J. V. Park, R. G. Griffin, J. A. Johnson, *Angew. Chem. Int. Ed.* **2017**, *56*, 188–192.
[46] A. V. Zhukhovitskiy, J. Zhao, M. Zhong, E. G. Keeler, E. A. Alt, P. Teichen, R. G. Griffin, M. J. A. Hore, A. P. Willard, J. A. Johnson, *Macromolecules* **2016**, *49*, 6896–6902.
[47] A. V. Zhukhovitskiy, M. Zhong, E. G. Keeler, V. K. Michaelis, J. E. P. Sun, M. J. A. Hore, D. J. Pochan, R. G. Griffin, A. P. Willard, J. A. Johnson, *Nat. Chem.* **2015**, *8*, 33–41.
[48] J. E. M. Lewis, *Chem. Eur. J.* **2021**, *27*, 4454–4460.
[49] J. E. M. Lewis, J. D. Crowley, *ChemPlusChem* **2020**, ***85***, 815–827.
[50] J. E. M. Lewis, A. Tarzia, A. J. P. White, K. E. Jelfs, *Chem. Sci.* **2020**, *11*, 677–683.
[51] S. S. Mishra, S. V. K. Kompella, S. Krishnaswamy, S. Balasubramanian, D. K. Chand, *Inorg. Chem.* **2020**, *59*, 12884−12894.
[52] D. Bardhan, D. K. Chand, *Chem. Eur. J.* **2019**, *25*, 12241–12269.
[53] S. Pullen, G. H. Clever, *Acc. Chem. Res.* **2018**, *51*, 3052–3064.
[54] W. M. Bloch, G. H. Clever, *Chem. Commun.* **2017**, *53*, 8506–8516.
[55] L. R. Holloway, P. M. Bogie, R. J. Hooley, *Dalton Trans.* **2017**, *46*, 14719–14723.
[56] R. Zhu, W. M. Bloch, J. J. Holstein, S. Mandal, L. V. Schäfer, G. H. Clever, *Chem. Eur. J.* **2018**, *24*, 12976–12982.
[57] W. M. Bloch, J. J. Holstein, W. Hiller, G. H. Clever, *Angew. Chem. Int. Ed.* **2017**, *56*, 8285–8289.
[58] D. Preston, J. E. Barnsley, K. C. Gordon, J. D. Crowley, *J. Am. Chem. Soc.* **2016**, *138*, 10578–10585.
[59] W. M. Bloch, Y. Abe, J. J. Holstein, C. M. Wandtke, B. Dittrich, G. H. Clever, *J. Am. Chem. Soc.* **2016**, *138*, 13750–13755.
[60] M. Yamashina, T. Yuki, Y. Sei, M. Akita, M. Yoshizawa, *Chem. Eur. J.* **2015**, *21*, 4200–4204.
[61] A- M. Johnson, R. J. Hooley, *Inorg. Chem.*, **2011**, **50**, 4671–4673.
[62] R.-J. Li, J. Tessarolo, H. Lee, G. H. Clever, *J. Am. Chem. Soc.* **2021**, *143*, 3865–3873.

[63] S. Sudan, R. Li, S. Jansze, A. Platzek, R. Rudolf, G. H. Clever, F. Fadaei Tirani, R. Scopelliti, K. Severin, *J. Am. Chem. Soc.* **2021**, *143*, 1773–1778.
[64] S. Prusty, K. Yazaki, M. Yoshizawa, D. K. Chand, *Chem. Eur. J.* **2017**, *23*, 12456–12461.
[65] P. Howlander, P. Das, E. Zangrando, P. S. Mukherjee, *J. Am. Chem. Soc.* **2016**, *138*, 1668–1676.
[66] Q.-F. Sun, S. Sato, M. Fujita, *Angew. Chem. Int. Ed.* **2014**, *53*, 13510–13513.
[67] D. Fujita, K. Suzuki, S. Sato, M. Yagi-Utsumi, Y. Yamaguchi, N. Mizuni, T. Kumasaka, M. Takata, M. Noda, S. Uchiyama, K. Kato, M. Fujita, *Nat. Commun.* **2012**, *3*, 1093.
[68] S. Sato, Y. Ishido, M. Fujita, *J. Am. Chem. Soc.* **2009**, *131*, 6064−6065.
[69] For the conversion of homoleptic into heteroleptic coordination cages by ligand substitution, see: J.-R. Li, H.-C. Zhou, *Nat. Chem.* **2010**, *2*, 893–898.
[70] P. Liao, B. W. Langloss, A. M. Johnson, E. R. Knudsen, F. S. Tham, R. R. Julian, R. J. Hooley, *Chem. Commun.* **2010**, *46*, 4932–4934.
[71] Z. He, W. Jiang, C. A. Schalley, *Chem. Soc. Rev.* **2015**, ***44***, 779–789.
[72] M. M. Safont-Sempere, G. Fernandez, F. Wurthner, *Chem. Rev.* **2011**, *111*, 5784–5814.
[73] B. Chen, J. J. Holstein, S. Horiuchi, W. G. Hiller, G. H. Clever. *J. Am. Chem. Soc.* **2019**, *141*, 8907−68913.
[74] N. M. Shivakumaraiah, N. Gowda, *J. Chem. Res.* **2005**, *2005*, 505–507.
[75] T. Harris, G. P. Gomes, S. Ayad, R. J. Clark, V. V. Lobodin, M. Tuscan, K. Hanson, I. V. Alabugin, *Chem* **2017**, *3*, 629–640.
[76] S. M. Jansze, K. Severin, *J. Am. Chem. Soc.* **2019**, *141*, 815−819.

Entry for the Table of Contents

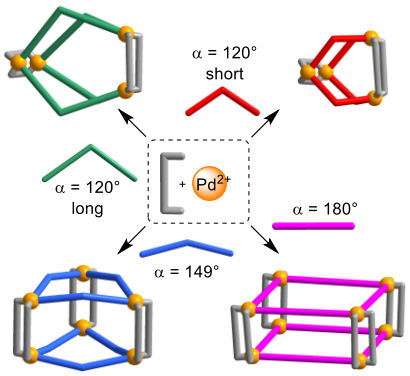

Heteroleptic Pd cages containing two types of dipyridyl ligands are described. The common feature of these complexes is the presence of two 1,3-di(pyridin-3-yl)benzene ligands (depicted in gray). By variation of the ligand bent angle α of the second ligand, we were able to able to increase the nuclearity of the assembly from 4 to 8.

Institute and/or researcher Twitter usernames: @kay_severin and @RujinL from @EPFL_CHEM_Tweet